Supplementary Information: Spatial predictors of response to immunotherapy in microsatellite stable metastatic colorectal cancer

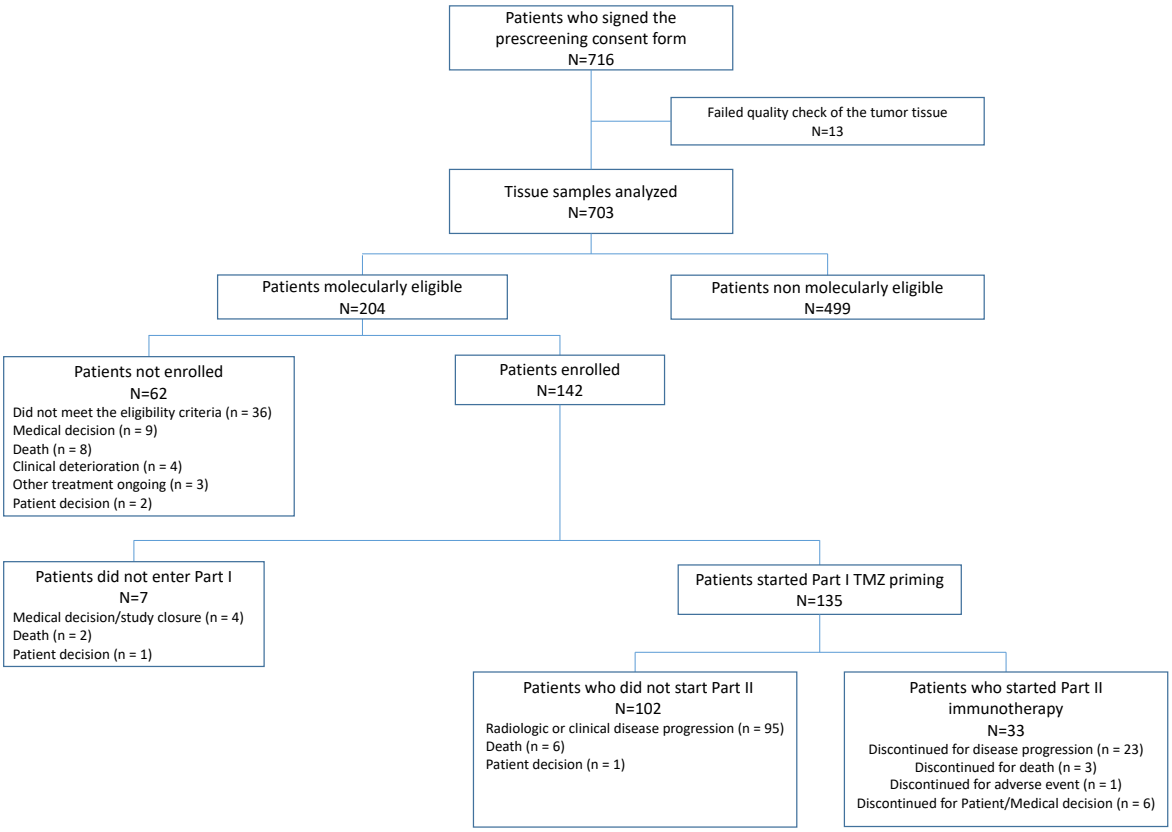

Supplementary Figure 1. Updated consort diagram

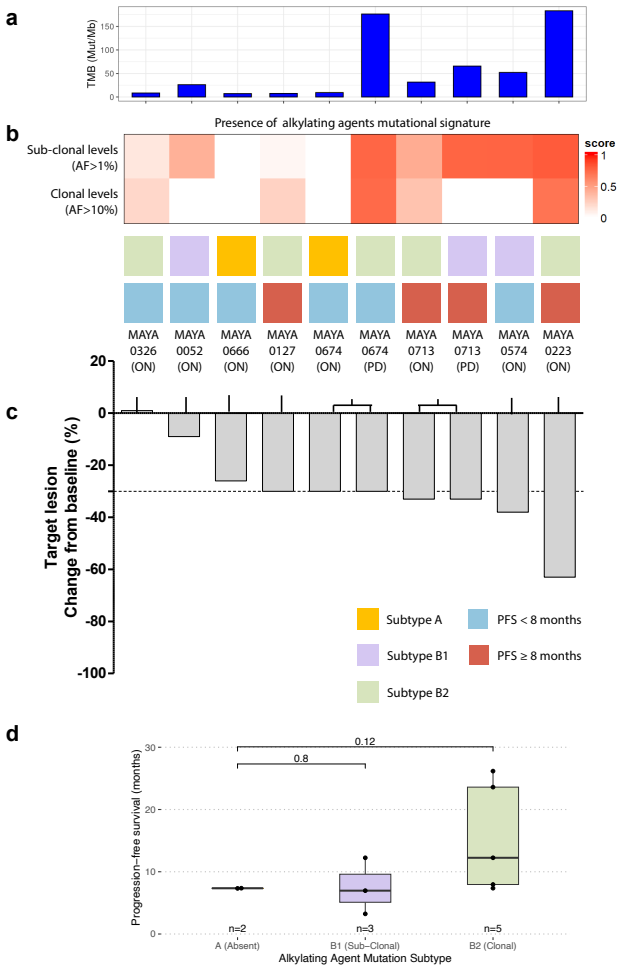

Supplementary Figure 2. Mutational signature and TMB analysis in biopsies after triplet

a, Barplot showing the tumor mutational burden estimated as number of non-synonymous mutations/Mb in tumor samples obtained from patients after treatment with triplet therapy (n=10). **b,** Heatmap showing the enrichment of the alkylating agents mutational signature (single base substitution 11 [SBS11]) occurring at sub-clonal levels (AF>1%) and clonal levels (AF>10%) in tumor samples obtained from patients after treatment with triplet therapy (n=10). Colors in heatmap represent the score output of MuSiCa (1). Patients were classified into three subtypes - A, B1, and B2 where subtype A corresponds to lack of the alkylating agents mutational signature, while B1 and B2 correspond to presence of the alkylating agents mutational signature at sub-clonal and clonal levels respectively. **c,** Barplot representing the changes (%) in the target lesions from baseline (n=10). Colored boxes indicate patients who had durable response (progression free survival >8 months [red]) or non-durable response (progression-free survival <8 months [blue]). **d,** Boxplot comparisons of PFS between patient subtypes A (n=2), B1 (n=3), and B2 (n=5). Data are presented as box plots showing the median (centre line), interquartile range (box limits: 25th and 75th percentiles). The two-sided Wilcoxon test was used.

Abbreviations: AF, allele frequency; ON, on-treatment tumor sample; PD, tumor sample obtained at time of progressive disease; TMZ, temozolomide; PFS , progression-free survival

Remarks: The alkylating agents mutational signature in samples treated with TMZ was previously described by Crisafulli et al (2). The mutational signature correlates with disease stabilization upon immune checkpoint inhibition.

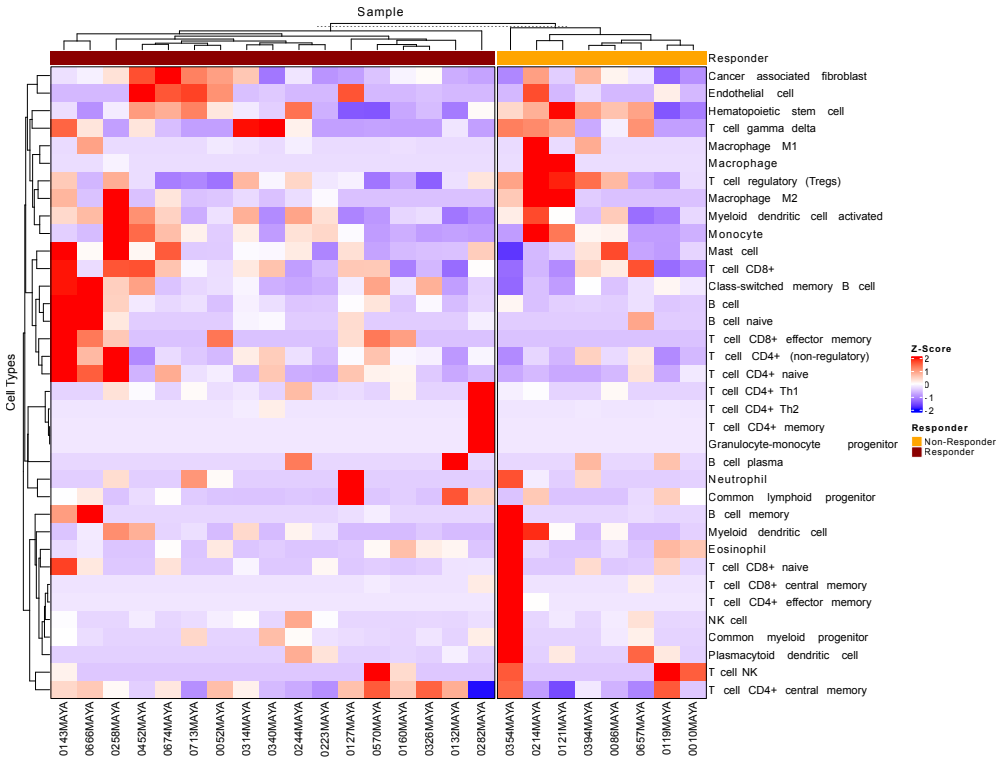

Supplementary Figure 3. **Immune cell composition of baseline tumors estimated by xCell deconvolution.**

Bulk RNA sequencing data from pre-treatment tumor samples were analyzed using the xCell algorithm to infer the relative enrichment of immune and stromal cell types. The heatmap displays xCell scores across individual patients, representing inferred abundance of immune subsets including T cells, B cells, macrophages, dendritic cells, and NK cells, as well as stromal components such as fibroblasts and endothelial cells. Scores are relative enrichment values rather than absolute proportions and are normalized across samples. Patients are grouped by response category [responder (R, n=17) vs non-responder (NR, n=8)]. The heatmap is descriptive, and no statistical testing is performed.

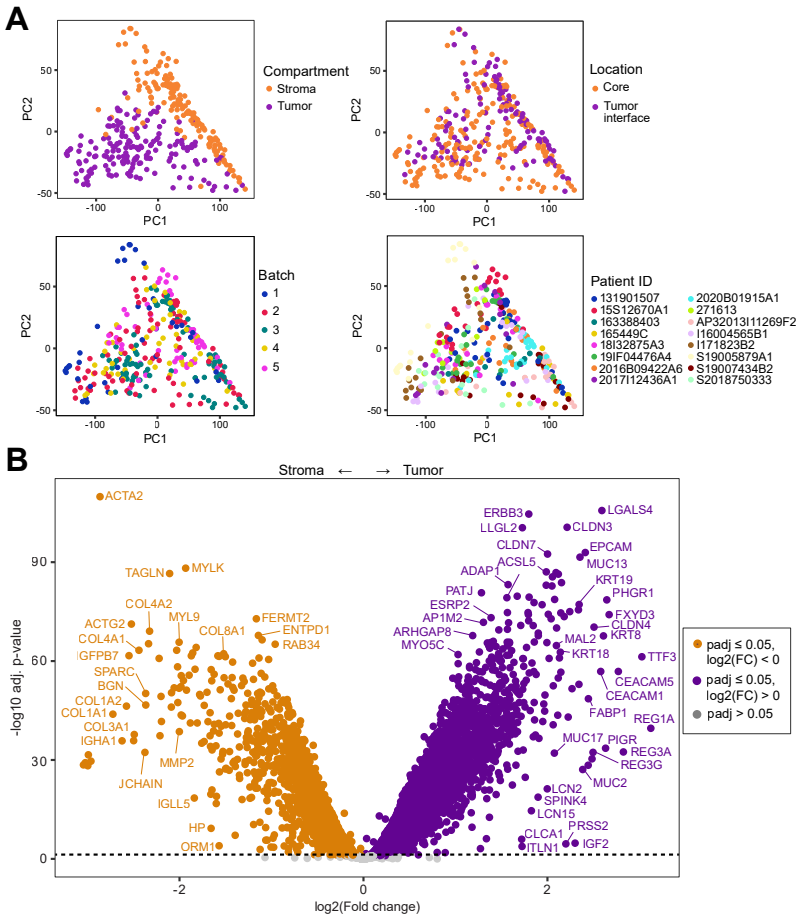

Supplementary Figure 4. Characteristics of Digital Spatial Profiling areas of illumination (AOIs).

a, Principal Component Analysis (PCA) dimension reduction of gene expression in areas of illumination (AOIs), colored according to labels shown (n=16). **b,** Volcano plot of differentially expressed gene analysis results of tumor AOIs vs. stroma AOIs (n=16). The dashed horizontal line marks p-value = 0.05.

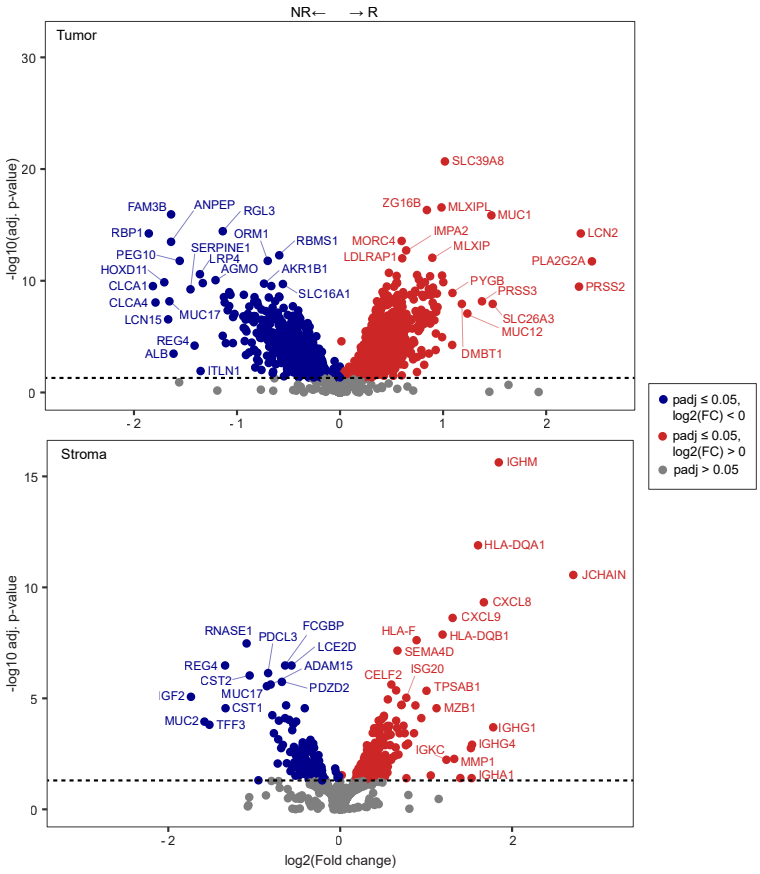

Supplementary Figure 5. Differential gene analysis results of responder vs. non-responder in tumor and stroma areas of illumination (AOIs).

Volcano plots of differentially expressed gene analysis results of responder tumor AOIs vs. non-responder tumor AOIs (above) and of responder stroma AOIs vs. non-responder stroma AOIs (below). Statistical significance is derived from negative binomial generalized linear models with Wald tests. P-values are adjusted for multiple testing using the Benjamini–Hochberg method, and adjusted p-values (FDR) are reported. The dashed horizontal line marks p-value = 0.05. Analyses were performed on tumor samples from responders (R, n = 8) and non-responders (NR, n = 8).

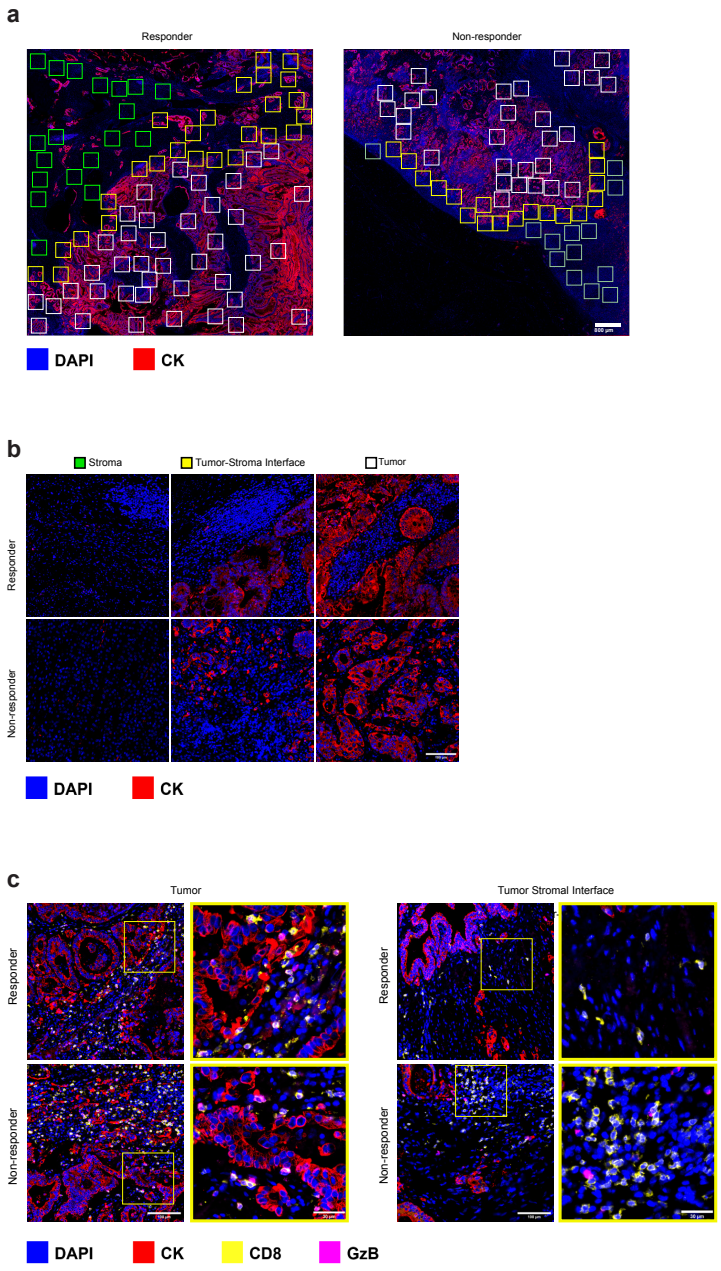

Supplementary Figure 6. Differential gene analysis results of responder vs. non-responder in tumor and stroma areas of illumination (AOIs).

a, Raw whole-slide images were segmented to define regions of interest (ROIs) within the tumor core, tumor–stroma interface (TSI), and stroma of a sample from a responder (n=1) and a non-responder (n=1). Images are stained with DAPI (blue) and cytokeratin (CK; red). Scale bar in white corresponds to 800 µm. **b,** Representative DAPI/CK-stained images across tumor, TSI, and stromal compartments in a responder (n=1) and a non-responder (n=1). Scale bar in white corresponds to 100 µm. **c,** Multiplex immunofluorescence images show paired ROIs from tumor and TSI regions with corresponding high-magnification insets (yellow boxes) from a responder (n=1) and a non-responder (n=1). Stains include DAPI (blue), CK (red), CD8 (yellow), and Granzyme B (magenta). Scale bars in white correspond to 100 µm for the main panels and 30 µm for high-magnification insets."

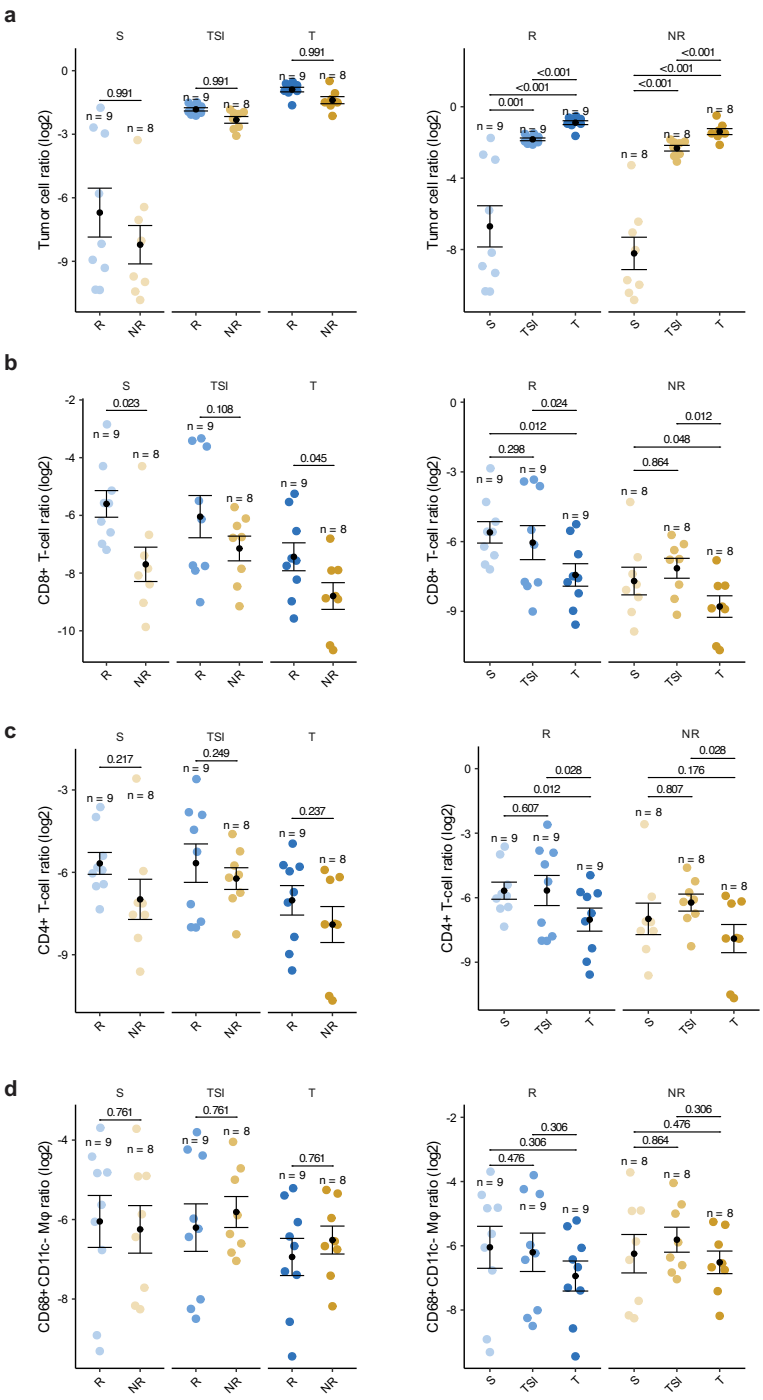

Supplementary Figure 7. Spatial proteomic analysis shows increased CD8+ T-cells at the tumor and stromal regions in responders compared to non-responders but no differences in populations of other immune cells.

a, Tumor cells defined as CK+/CD45-/CD68-/CD11c- cells were present in increasing proportions between the stroma, TSI and tumor regions in both responders (R, n=9) and non-responders (NR, n=8). **b,** Increased CD8+ T-cells at the tumor and stromal regions in responders (R, n=9) compared to non-responders(NR, n=8). **c,** No differences in populations of CD4+ T-cells were present within the regions between responders (R, n=9) and non-responders (NR, n=8). **d,** No differences in populations of CD68+ macrophages were present within the regions between responders (R, n=9) and non-responders (NR, n=8). Data points represent individual samples; bars denote mean ± SEM. P-values were calculated

using unpaired t-tests comparing R vs NR at each timepoint, and adjusted for multiple comparisons using the Benjamini–Hochberg (BH) method.

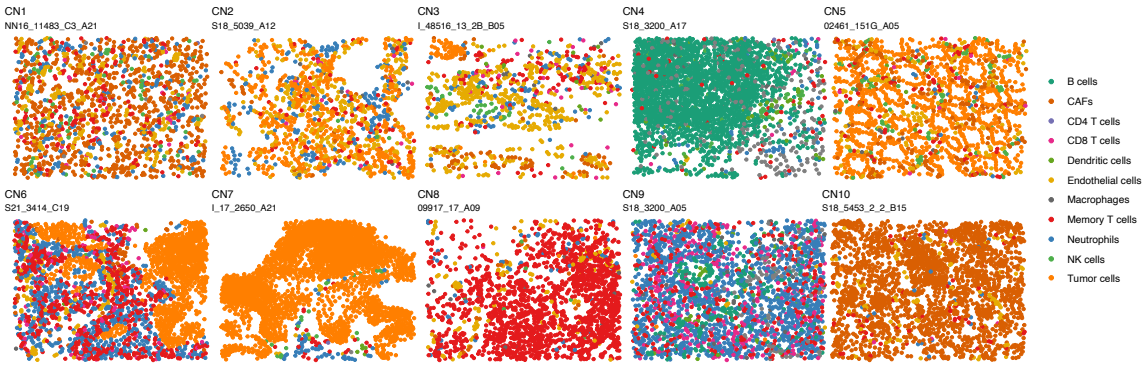

Supplementary Figure 8. Overview representative regions of interests for spatially identified cellular neighborhoods

Abbreviations: CN, cellular neighborhood.

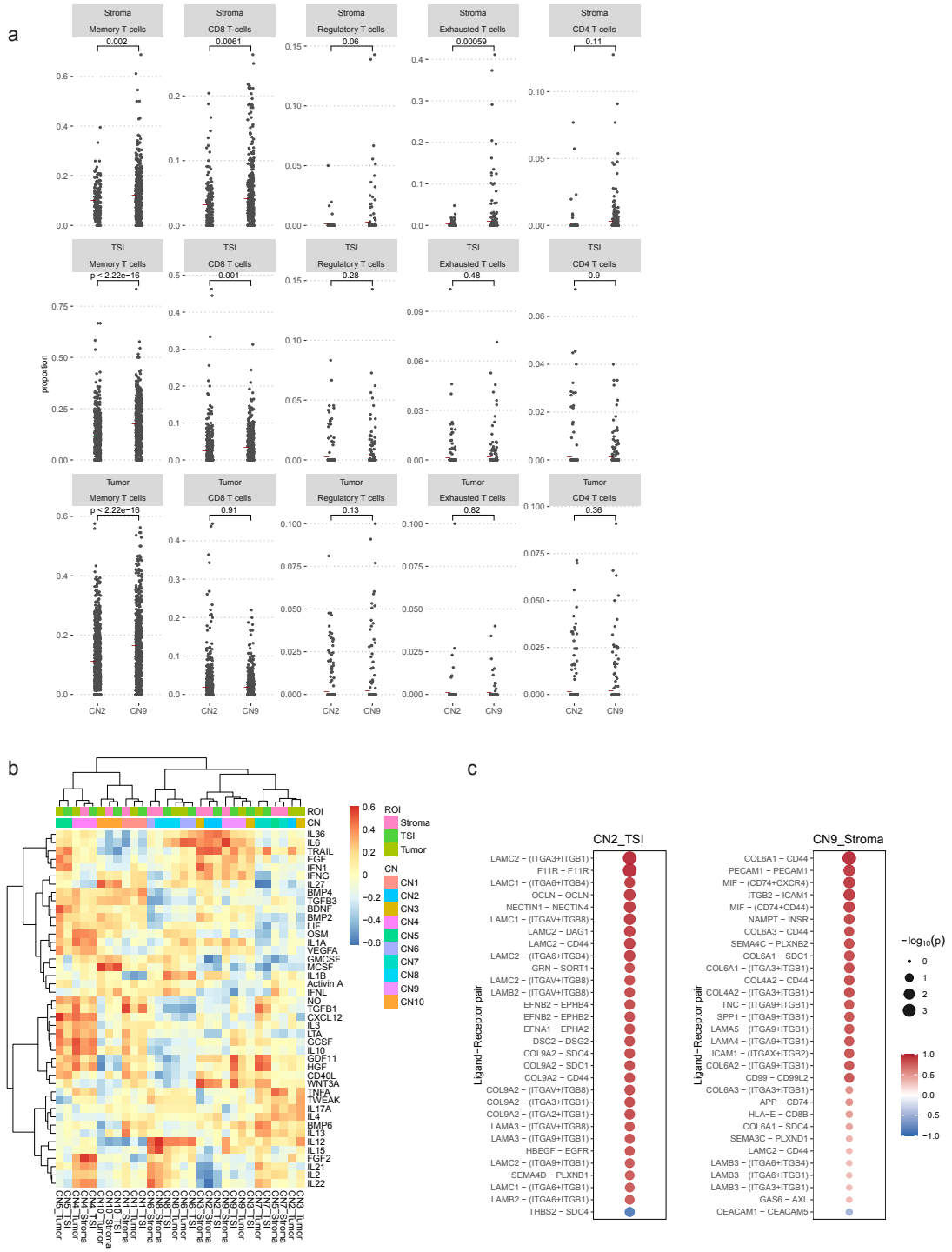

Supplementary Figure 9. Functional correlates of CN2 and CN9 across immune composition, cytokine profiles, and ligand–receptor interactions

a, Comparisons of T cell subtype proportions between CN2 and CN9 stratified by region of interest (n=26 samples from n=26 patients). The two-sided t-test was used. **b,** Heatmap of Pearson correlation between CN proportions per ROI against cytokine z-scores (CytoSig) (n=45 samples from n=26 patients). **c,** Ligand–receptor correlations with CN2 and CN9 across compartments (n=6 samples). Bubble plot showing Spearman correlations between CellChat-inferred ligand–receptor interaction scores and CN2 or CN9 proportions in the stroma and tumor–stroma interface (TSI). Red indicates positive and blue negative correlations. Bubble size reflects the nominal statistical significance.

Abbreviations: CN, cellular neighborhood; TSI, tumor stromal interface; ROI, region of interest

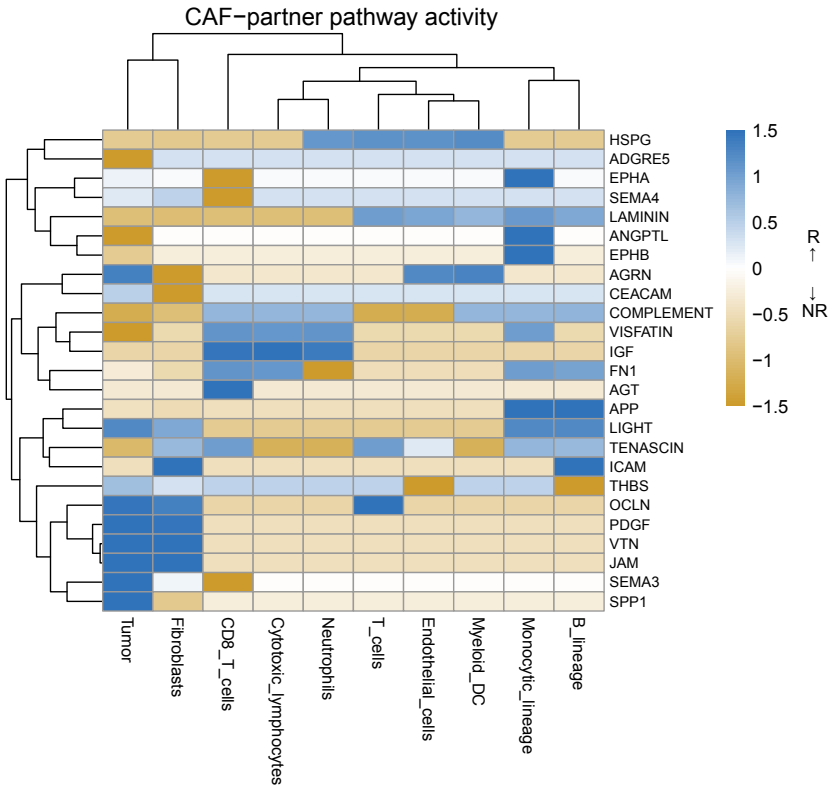

Supplementary Figure 10. CAF–partner pathway differences between responders and non-responders.

Heatmap of $\log_2$ fold-change (R/NR) in CAF–partner ligand–receptor activity collapsed to pathway families. Each row represents a pathway, and each column represents a partner cell type. Blue indicates relative enrichment in responders (n=4), while gold indicates relative enrichment in non-responders (n=3).

Abbreviations: R, responders; NR, non-responders; CAF, cancer-associated fibroblast

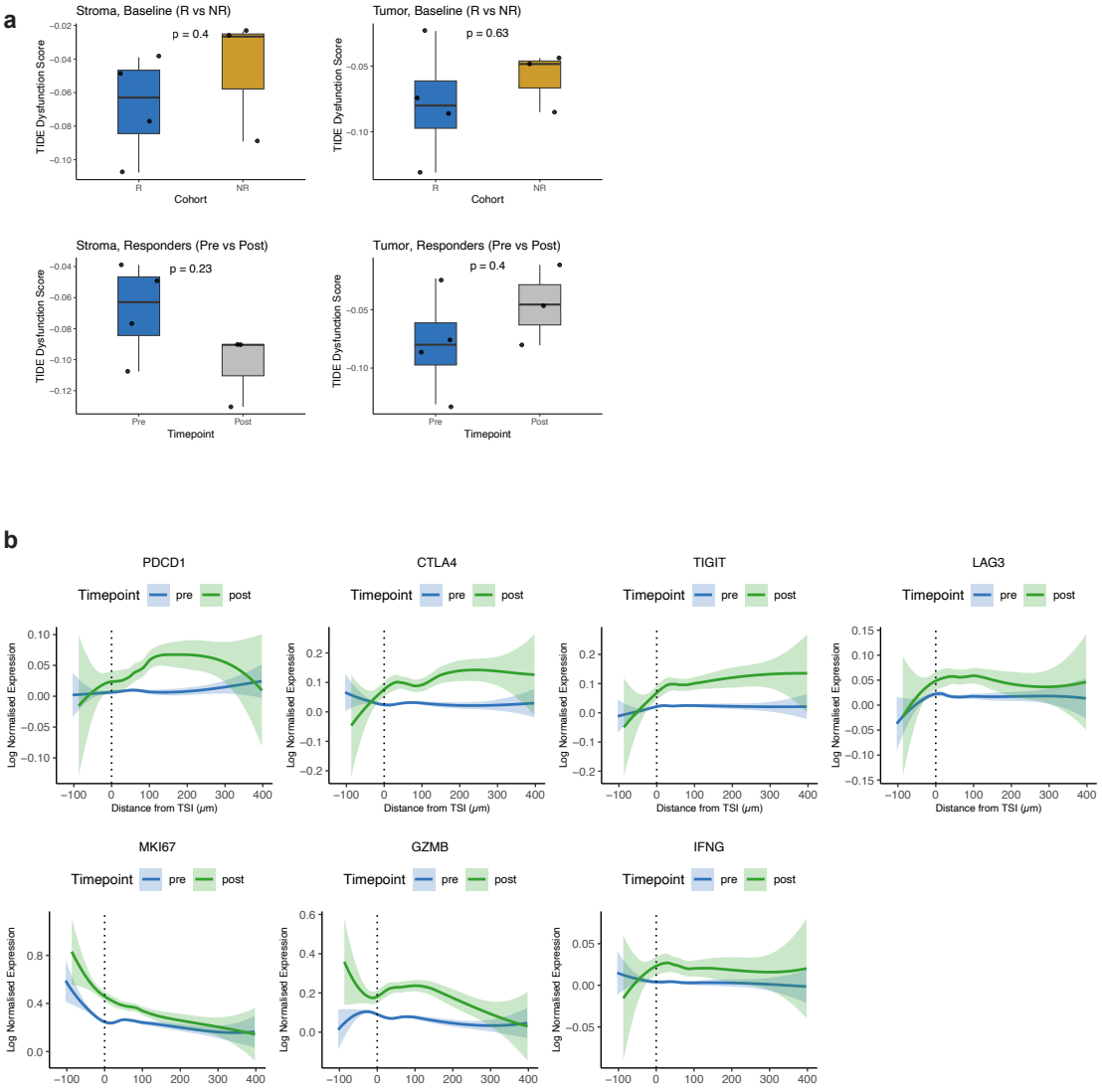

Supplementary Figure 11. CD8⁺ T Cell Dysfunction and Exhaustion Across Tumor and Stromal Compartments

a, CD8⁺ T cell dysfunction scores tumor and stromal regions in responders and non-responders, pre- and post-treatment. Post-treatment samples were only available for three patients, all of whom were responders. T cell dysfunction was estimated using the TIDE-derived Dysfunction score. Data are presented as box plots showing the median (centre line), interquartile range (box limits: 25th and 75th percentiles), and whiskers extending to 1.5× the interquartile range from the quartiles. Group differences were assessed using a two-sided Wilcoxon rank-sum test across across non-responder pre-treatment samples (n = 3), responder pre-treatment samples (n = 4), and responder post-treatment samples (n = 3). **b,** Spatial gene expression gradients of CD8⁺ T cell exhaustion and activation markers across the tumor–stroma axis. Smoothed conditional means density curves were retrieved with the geom_smooth() function in ggplot2 in R, based on pooled spot-level expression data from responder pre-treatment samples (n = 4), and responder post-treatment samples (n = 3). The solid line represents the smoothed conditional mean, and the shaded band indicates the 95% confidence interval of the fitted curve.

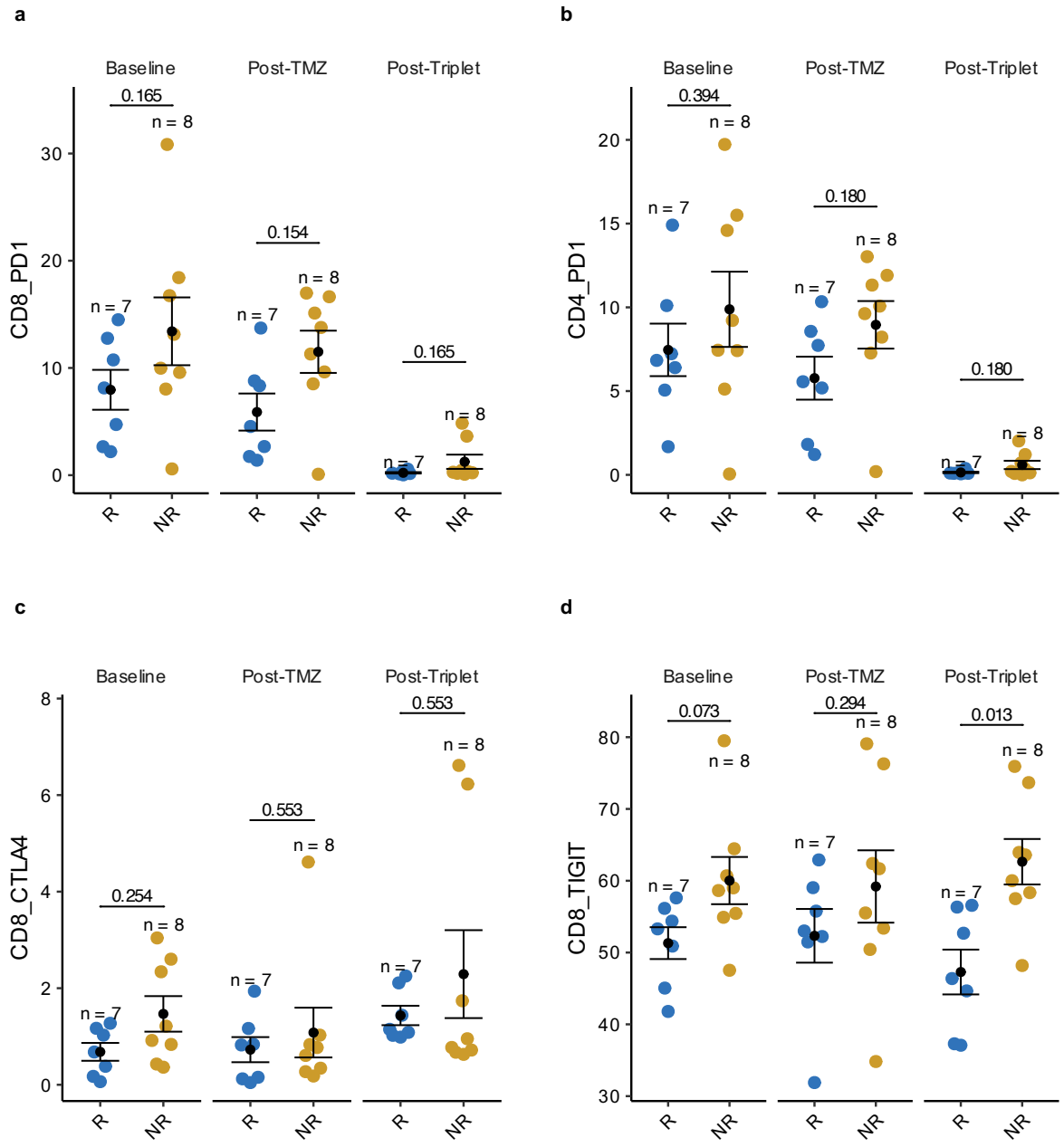

Supplementary Figure 12. Peripheral immune cell phenotypes at static timepoints by flow cytometry

Flow cytometric analysis of peripheral blood mononuclear cells (PBMCs) was performed at baseline, post-temozolomide (Post-TMZ), and post-triplet therapy timepoints in patients treated on the study. Plotted are the frequencies of **a,** $CD8^+PD\text{-}1^+$, **b,** $CD4^+PD\text{-}1^+$, **c,** $CD8^+CTLA\text{-}4^+$, and **d,** $CD8^+TIGIT^+$ T cells, stratified by responder (R, blue, n=7) and non-responder (NR, yellow, n=8) status. Data points represent individual patients; bars denote mean ± SEM. P-values were calculated using unpaired t-tests comparing R vs NR at each timepoint.

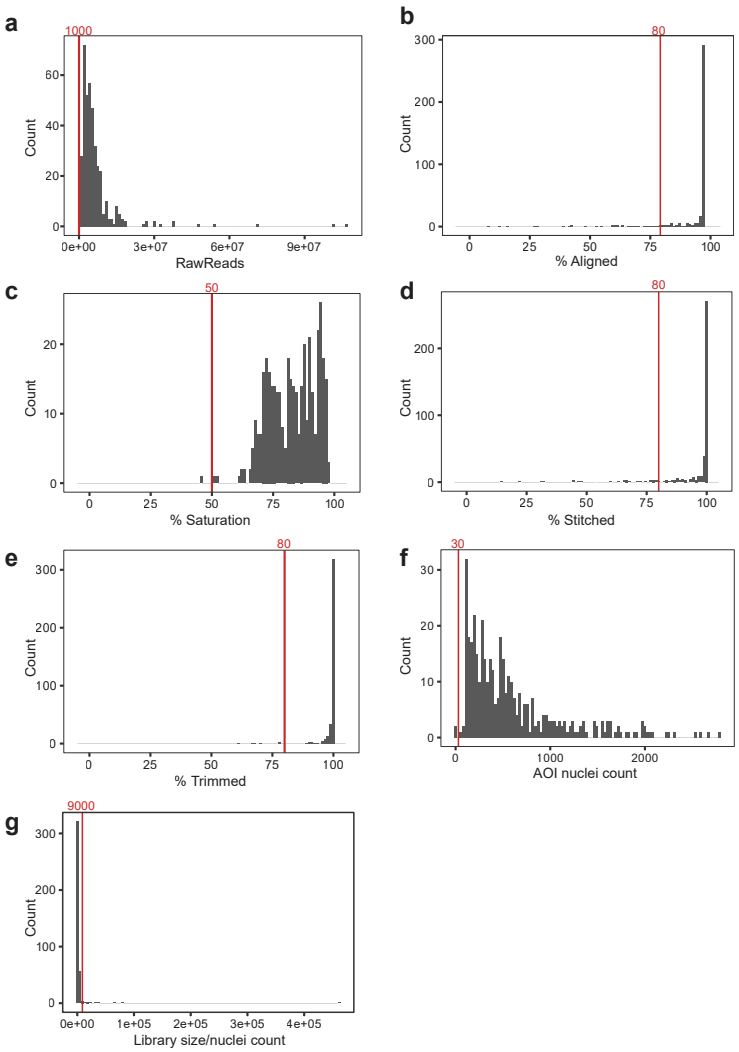

Supplementary Figure 13. Digital Spatial Profiling areas of illumination (AOI) quality metrics.

Histograms of raw read counts **a**, percentage of aligned reads **b**, percentage of read saturation **c**, percentage of stitched reads **d**, percentage of trimmed reads **e**, nuclei count in AOI **f**, library size to nuclei count ratio **g,** Red vertical lines mark minimum quality control threshold in a, b, c, d, e, and f, and mark maximum threshold in g.

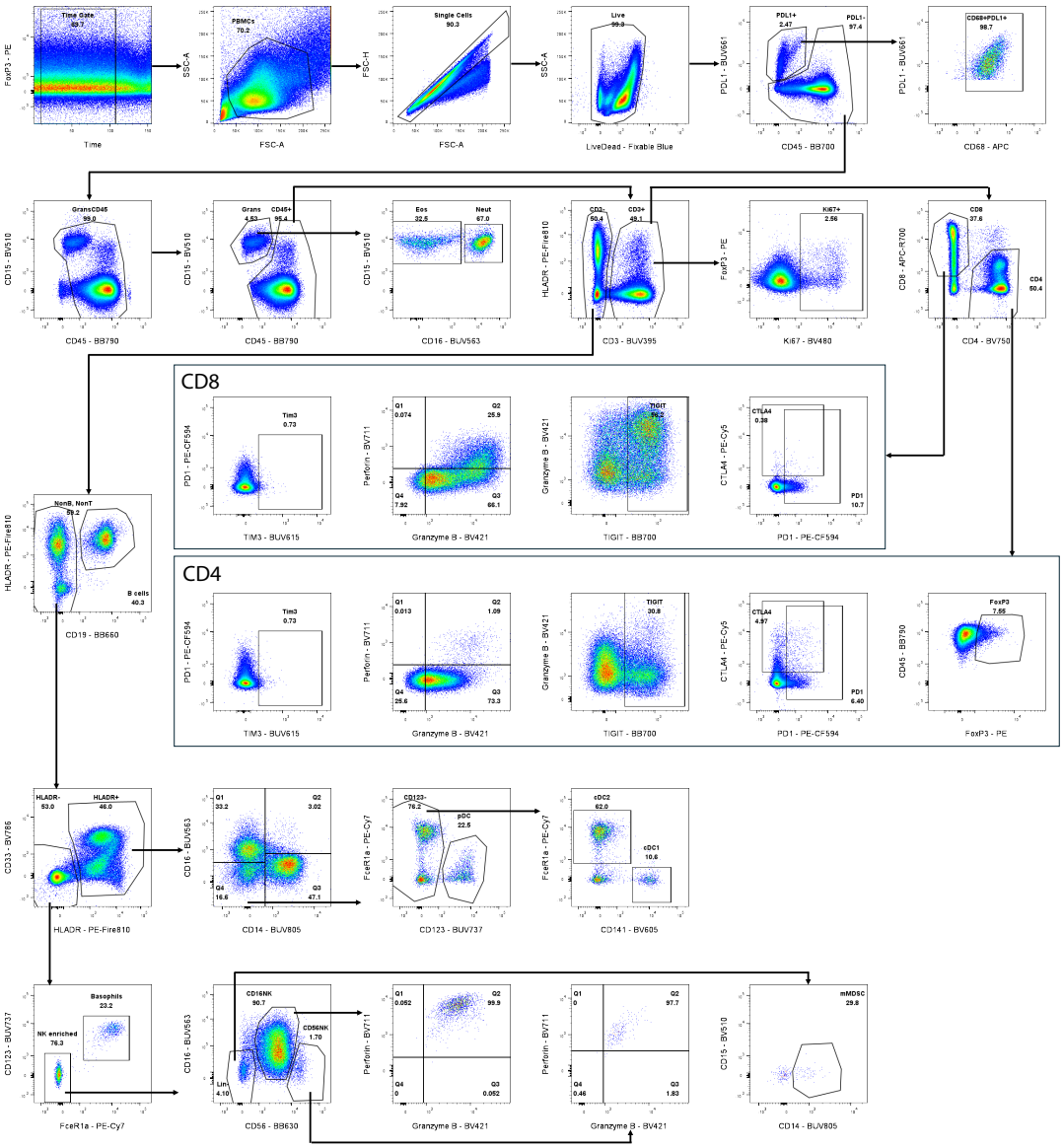

Supplementary Figure 14. Flow cytometry gating strategy

Cell type	*Subtype*	*Positive marker*	*Additional marker for subtyping*	*Negative marker*
B cells	B cells	CD19 or CD20		CD3; CK
Dendritic cells	Dendritic cells	CD11c		CD3; CD20; CK
Endothelial cells	Endothelial cells	CD31		CD45; CK
Cancer-Associated Fibroblasts	Cancer-Associated Fibroblasts	aSMA		CK; CD68; CD31; CD45
Macrophages	M1 Macrophages	CD68	HLA-DR; CD11c	CD163; CK
Macrophages	M2 Macrophages	CD68	CD163	HLA-DR; CK; CD11c
NK cells	Activated NK cells	CD56	GZMB	CD3; CD20; CK
NK cells	NK cells	CD56		CD3; CD20; CK
Neutrophils	Neutrophils	CD16		CD3; CD20; CK
Exhausted T cells	Early-stage exhausted T cells	CD3+PD-1		CK; LAG-3
Exhausted T cells	Terminally exhausted T cells	CD3+LAG-3		CK
CD8 T cells	Proliferating CD8 T cells	CD8	Ki67	CD4; CD20; CK; GZMB
CD8 T cells	Effector Cytotoxic T Cells	CD8	GZMB	CD4; CD20; CK; Ki67
CD8 T cells	CD8 T cells	CD8		CD4; CD20; CK; Ki67; GZMB; LAG-3; PD-1
CD4 T cells	T-helper cells	CD3+CD4		CD8; CD20; CK
Regulatory T cells	Regulatory T cells	CD3+FOXP3		CD8; CD20; CK
Memory T cells	Memory T cells	CD3	CD45RO	CD20; CK
Tumor cells	Tumor cells	CK		CD45

Supplementary Table 1. Markers utilized for cell type identification on Lunaphore

Abbreviations: NK, natural killer

Remarks: Cells were retrieved utilizing a combination of markers as shown above. For example, B cells were denoted by CD19+CD3-CK- or CD20+CD3-CK-.

No	Marker	Clone	Company	Catalogue	Dilution
1	aSMA	1A4	Cell Marque	202M-96	1:2000
2	BDCA-2	10E6.1	Merck	MABF94	1:100
3	CD11b	EPR1344	Abcam	ab133357	1:2000
4	CD11c	EP1347Y	Abcam	ab52632	1:3000
5	CD14	EPR3653	Abcam	ab133335	1:2000
6	CD15	Carb-3	Dako	M363101-2	1:500
7	CD16	SP175	Cell Marque	116R-16	1:1500
8	CD163	MRQ-26	Cell Marque	163M-15	1:80
9	CD19	EPR5906	Abcam	ab134114	1:1500
10	CD20	SP32	Thermo	MA1-39416	1:100
11	CD21	EP3093	Cell Marque	121R-16	1:1000
12	CD3	MRQ-39	Cell Marque	103R-96	1:200
13	CD31	EP3095	Abcam	ab134168	1:4000
14	CD34	EP88	Cell Marque	134R-16	1:4000
15	CD38	SP149	Cell Marque	118R-15-RUO	1:100
16	CD39	EPR20627	Abcam	ab223842	1:3000
17	CD4	EPR6855	Abcam	ab133616	1:1000
18	CD45	2B11 + PD7/26	Dako	M070101-2	1:150
19	CD45RA	HI100	BioLegend	304102	1:3000
20	CD45RO	UCHL1	Dako	M074201-2	1:1000
21	CD56	MRQ-42	Cell Marque	156R-95	1:5000
22	CD68	KP1	Thermo	MA5-13324	1:500
23	CD8	4B11	BioRad	MCA1817T	1:250
24	CK	AE1/AE3	Dako	M351501-2	1:150
25	E-Cadherin	36/E-Cadherin (RUO)	BD Bioscience	610182	1:1000
26	Eomes	WD1928	Invitrogen	14-4877-82	1:200
27	FoxP3	SP97	Thermo	MA5-16365	1:200
28	GZMB	EPR20129-217	Abcam	ab208586	1:2000
29	HLA-DR	TAL 1B5	Santa cruz	sc-53319	1:2000
30	ICOS	EPR20560	Abcam	ab224644	1:100
31	IDO-1	V1NC3IDO	Invitrogen	14-9750-82	1:3000
32	Ki67	MIB-1	Dako	M724001-2	1:1500
33	LAG-3	17B4	NovusBio	NBP1-97657-100	1:8000
34	Lamin A	133A2	Thermo	MA1-06101	1:200
35	PD1	EPR4877(2)	Abcam	ab137132	1:6000
36	PD-L1 (73-10)	73-10	Abcam	ab228415	1:2000
37	Podoplanin	D2-40	Dako	M361929-2	1:50
38	S100	4C4.9	Thermo	MA5-12969	1:100
39	Tryptase	AA1	BioLegend	369402	1:10000
40	VISTA	D1L2G	Cell Signalling	64953	1:150

Supplementary Table 2. Antibody list for the COMET staining panel

S/N	Fluorophore	Marker	Company	Dilution
	Surface markers			
1	BB630	CD56	BD Biosciences	1:100
2	BB660	CD19	BD Biosciences	1:100
3	BB700	TIGIT	BD Biosciences	1:50
4	BB790	CD45	BD Biosciences	1:200
5	BUV395	CD3	BD Biosciences	1:50
6	BUV496	Live Dead	Thermofisher	1:100
7	BUV563	CD16	BD Biosciences	1:50
8	BUV615	TIM3	BD Biosciences	3:100
9	BUV661	PD-L1	BD Biosciences	1:50
10	BUV737	CD123	BD Biosciences	1:50
11	BUV805	CD14	BD Biosciences	1:50
12	APC-R700	CD8	BD Biosciences	1:50
13	R718	CD206	BD Biosciences	1:50
14	APC-Vio770	CD172a	Miltenyi Biotec	3:100
15	Pe-CF594	PD1	BD Biosciences	1:50
16	Pe-Cy7	FceR1a	Biolegend	1:50
17	Pe-Fire810	HLA-DR	Biolegend	1:50
18	BV510	CD15	BD Biosciences	1:50
19	BV570	CD11b	Biolegend	1:25
20	BV605	CD141	BD Biosciences	1:50
21	BV750	CD4	BD Biosciences	1:200
22	BV786	CD33	BD Biosciences	1:50
	Intracellular markers			
23	FITC	IDO	eBioscience	1:20
24	APC	CD68	Miltenyi Biotec	1:50
25	PE	Foxp3	BD Biosciences	1:5
26	Pe-Cy5	CTLA4	BD Biosciences	1:50
27	BV421	GZMB	BD Biosciences	1:100
28	BV480	Ki67	BD Biosciences	1:50
29	BV711	Perforin	Biolegend	1:100

Supplementary Table 3. Antibody panel for peripheral flow cytometry

Supplementary References

1. Díaz-Gay M, Vila-Casadesús M, Franch-Expósito S, Hernández-Illán E, Lozano JJ, Castellví-Bel S. Mutational Signatures in Cancer (MuSiCa): a web application to implement mutational signatures analysis in cancer samples. BMC bioinformatics. 2018;19(1):224.
2. Crisafulli G, Sartore-Bianchi A, Lazzari L, Pietrantonio F, Amatu A, Macagno M, et al. Temozolomide Treatment Alters Mismatch Repair and Boosts Mutational Burden in Tumor and Blood of Colorectal Cancer Patients. Cancer discovery. 2022;12(7):1656-75.